PERGAMON

Computerized Medical Imaging and Graphics 25 (2001) 265–275

Computerized Medical Imaging and Graphics

www.elsevier.com/locate/compmedimag

A multiscale optimization approach for the dynamic contour-based boundary detection issue

M. Mignotte*, J. Meunier[1]

Département d'Informatique et de Recherche Opérationnelle, DIRO, P.O. Box 6128, Succursalle Centre-ville, Montréal, Québec, Canada H3C 3J7

Received 13 April 2000; accepted 18 September 2000

Abstract

We present a new multiscale approach for deformable contour optimization. The method relies on a multigrid minimization method and a coarse-to-fine relaxation algorithm. This approach consists in minimizing a cascade of optimization problems of reduced and increasing complexity instead of considering the minimization problem on the full and original configuration space. Contrary to classical multi-resolution algorithms, no reduction of image is applied. The family of defined energy functions are derived from the original (full resolution) objective function, ensuring that the same function is handled at each scale and that the energy decreases at each step of the deformable contour minimization process. The efficiency and the speed of this multiscale optimization strategy is demonstrated in the difficult context of the minimization of a region-based contour energy function ensuring the boundary detection of anatomical structures in ultrasound medical imagery. In this context, the proposed multiscale segmentation method is compared to other classical region-based segmentation approaches such as Maximum Likelihood or Markov Random Field-based segmentation techniques. We also extend this multiscale segmentation strategy to active contour models using a classical edge-based likelihood approach. Finally, time and performance analysis of this approach, compared to the (commonly used) dynamic programming-based optimization procedure, is given and allows to attest the accuracy and the speed of the proposed method.

Keywords: Active contour model; Snake; Multiscale optimization; Boundary-based segmentation; Ultrasound medical images

1. Introduction

Segmentation remains a necessary step in medical imaging to obtain qualitative measurements such as the location of objects of interest as well as for quantitative measurements such as area, volume or the analysis of dynamic behaviour of anatomical structures over time. Among these images, ultrasound images play a crucial role, because they can be produced at video-rate and therefore allow a dynamic analysis of moving structures. Moreover, the acquisition of these images is non-invasive, cheap, and does not require ionizing radiations compared to other medical imaging techniques. On the other hand, the automatic segmentation of anatomical structures in ultrasound imagery is a real challenge due to acoustic interferences (speckle noise) and artifacts which are inherent in these images. These artifacts, caused by turbulent blood flow, multiple reverberations, non-rigid deformation of observed anatomical structures, air in the lungs, ribs, etc., create open contours and/or ill defined boundaries, making ineffective algorithms such as classical maximum likelihood (ML) or Markov random field-based segmentation techniques [1,2].

Among the existing segmentation techniques, the active contour models, or so-called *snakes* [3], are an effective way to overcome these artifacts and to rightly model the fact that the object to be detected is assumed to be connected. Besides, their ability to efficiently combine both the available a priori knowledge about the structure of interest (generally a smoothness constraint) and local correspondences with the image features (such as the grey level statistical distribution inside and outside the object), makes them very attractive for the segmentation task in ultrasound imagery. Nevertheless, this modelling finally requires to solve an intricate energy function minimization problem. The configuration space of this optimization problem is generally *very large* and the resulting energy function may exhibit many local *minima*, especially when the image contains strong noise, which is frequently the case

* Corresponding author. Tel.: +1-514-343-6111, ext. 1657; fax: +1-514-343-5834.

E-mail addresses: mignotte@iro.umontreal.ca (M. Mignotte), meunier@iro.umontreal.ca (J. Meunier).

[1] Tel.: +1-514-343-7107; fax: +1-514-343-5834.

0895-6111/01/$ - see front matter
PII: S0895-6111(00)00075-6

in ultrasound imagery. In order to cope with this optimization problem, gradient-based methods have originally been proposed [3]. The main drawback of these techniques is to require a proper initialization of the initial contour not *too far* from the expected boundary, otherwise they will converge towards bad local *minima*. dynamic programming (DP) [4] can solve the optimality problem, although at the expense of a very high computational load. In order to shorten execution times, researchers have recently suggested to combine gradient or DP-based methods with a multiresolution framework [5]. Nevertheless, the optimal solution is no more guaranteed. Besides, the construction of the "multiresolution pyramid" results in losing some important information that the energy function to be minimized is sensitive to.

In order to overcome these above mentioned problems, we propose herein to extend, to our minimization problem, the multiscale optimization strategy combined with the multiresolution framework introduced in Ref. [6] for the estimation of the optical flow in an image sequence. The key idea of this strategy consists in minimizing the global energy function through an appropriate hierarchy of subspaces of the whole configuration space. These subspaces contain constrained configurations describing the expected solution at different scales. In our application, these solutions are modelled as being the optimal positions of a sequence of dynamic contour models, of decreasing thickness, whose energy function is derived from the original energy function. This constrained optimization is implemented using a coarse-to-fine procedure on a pyramidal structure. This multiscale method has shown to be very robust for optimizing highly non-linear objective functions and has turned out to provide quickly good estimates very close to the global *minima* [6].

This paper is organized as follows. Section 2 presents the dynamic contour model used in a region and edge-based segmentation approach and the resulting energy functions to be optimized in these two cases. Section 3 recalls the DP-based optimization procedure commonly used to tackle this problem. The proposed multiscale minimization strategy adapted to these two problems is described in Section 4. In Section 5, we report some experimental results on synthetic and real ultrasound and radiographic medical images. Finally, Section 6 contains concluding remarks and perspectives.

2. The active contour model

The active contour model (or *snake*), introduced by Kass et al. in Ref. [3], formulates the boundary detection issue as an energy function minimization problem. Formally, an active contour V is simply defined by an ordered set of n nodes, $V = [v_1, v_2, \ldots, v_n]$, giving coordinates of points on the contour in a circular manner. A cubic B-spline curve involving these n control points (or a simple straight line between each node) allows to completely define this model. Given an input image y, its energy function is generally given by,

$$E_{\text{snake}}(V) = \sum_{i=1}^{n} (E_{\text{int}}(v_i) + \beta E_{\text{ext}}(v_i, y)), \tag{1}$$

where β is a weighting parameter. E_{int} and E_{ext} are the internal and external energy terms, respectively, also called the constraint forces, of the contour element v_i. These two energy terms play different roles in the energy minimization process. The internal energy allows to express the available a priori knowledge about the contour shape to be detected whereas the external energy allows to pull the snake towards the desired image features [3] (such as edges, regions, or both [7], textures, etc.). The definition of these energy terms have to be carefully defined according to the application and the input image. Let us finally add that the use of such global energy-based models fall into the Bayesian framework [8].

In order to model our a priori knowledge on the smoothness of the anatomical shape boundary to be detected, a commonly used solution consists in measuring the curvature at each node of the contour [9] and then in using this measure as the internal energy term, i.e.

$$E_{\text{int}}(v_i) = \arccos\left(\frac{\overrightarrow{v_{i-1}v_i} \cdot \overrightarrow{v_i v_{i+1}}}{\|\overrightarrow{v_{i-1}v_i}\| \cdot \|\overrightarrow{v_i v_{i+1}}\|} \right), \tag{2}$$

that is the angle between the two vectors $\overrightarrow{v_{i-1}v_i}$ and $\overrightarrow{v_i v_{i+1}}$. $\|\vec{v}\|$ is the norm of the vector $\vec{v}$ and "$\cdot$" represents the dot product between two vectors. In the minimization process, this a priori energy term penalizes high curvature on the contour.

In a commonly used active contour model-based segmentation approach, spatial gradient measures derived from the input image y, are generally exploited in the external (or likelihood) energy term [8]. This energy term can be defined by,

$$E_{\text{ext}}(v_i, y) = -\|\nabla y(v_i)\|, \tag{3}$$

which defines external energy as the negative of the image gradient ∇y at v_i. In order to pull the snake towards the right edges and to improve the detection results, we can also make the external energy sensitive to the tangent angle of the contour at v_i [10].

In ultrasound imagery, due to the speckle noise and artifacts which are inherent to acoustic images, our external energy term cannot rely efficiently on this type of measure. An alternative model consist in exploiting the statistical distribution of the grey levels inside and outside the boundary of the object to be detected [11]. Let $y = \{y_s \in S\}$, the set of pixels of the image located on a lattice S of M sites s. Assuming one probability density function (PDF), $P_{\text{in}}(\cdot)$, for the pixels inside the object and another PDF, $P_{\text{out}}(\cdot)$, for the pixels outside the object, we can then define the following

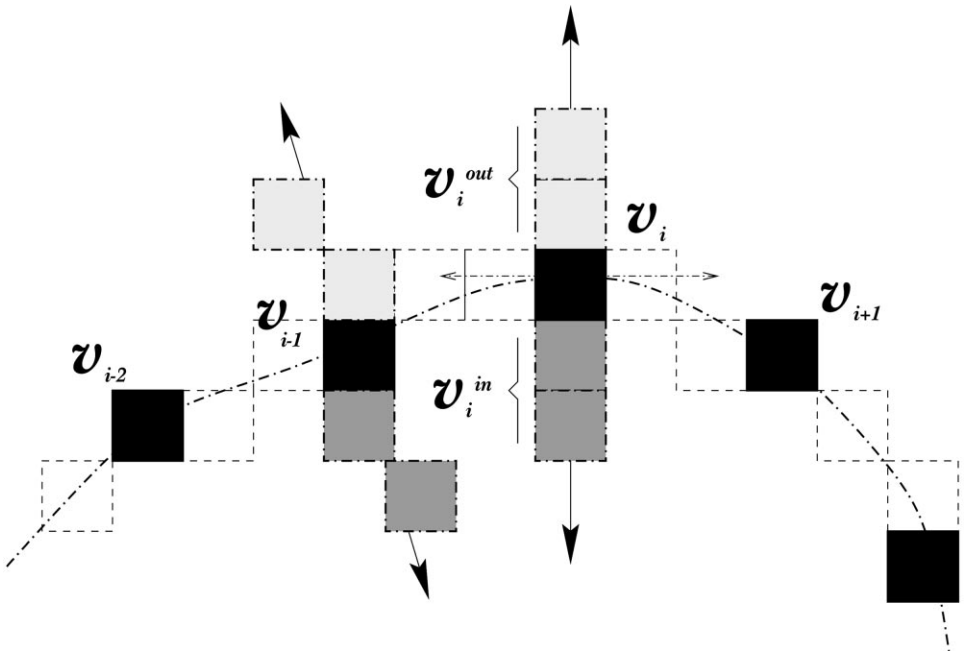

Fig. 1. Portion of a contour model showing five connected nodes and the set of points v_i^{in} and v_i^{out} used in the external energy term. $N_{\text{in}} = N_{\text{out}} = 2$ in this example.

external energy term by:

$$E_{\text{ext}}(v_i, y) = -\frac{1}{N_{\text{in}}} \sum_{s \in v_i^{\text{in}}} \ln P_{\text{in}}(y_s) - \frac{1}{N_{\text{out}}} \sum_{s \in v_i^{\text{out}}} \ln P_{\text{out}}(y_s), \tag{4}$$

where y_s designates the grey level of the pixel at site s. The summation of the first and second term of E_{ext} is over all the N_{in} and N_{out} selected points belonging to the straight segment perpendicular to the contour at node v_i, passing through this point, and, respectively, located inside and outside the contour, as shown in Fig. 1. This likelihood term is minimal when the snake delineates two homogeneous regions, at node v_i, distributed according to the grey level statistical distribution corresponding to each region.

Using these two energy terms, the optimal contour, V_{opt}, can then be obtained by finding the one that minimizes the energy $E_{\text{snake}}(V)$, i.e.

$$V_{\text{opt}} = \arg \min_{\{v_i\}} E_{\text{snake}}(V). \tag{5}$$

where $\{v_i\}$ designates the set of nodes that minimizes the snake energy (i.e. the optimal contour). Unfortunately, minimizing such a global energy function is often an intricate problem: the space of possible contours Ω is generally *very large* and the energy function may exhibit many local *minima*, especially when the image contains strong noise, which is frequently the case in ultrasound imagery (see Section 5).

3. Snake optimization methods

In Ref. [3] and in many other works, gradient-based methods are used for the energy minimization of this energy function type. These methods are simple but have the disadvantage to require a proper initialization of the dynamic contour not *too far* from the expected boundary, otherwise they will converge toward bad local *minima*. In order to overcome this problem, stochastic methods based on simulated annealing (SA) [8] have then been proposed. These ones have the capability of avoiding local *minima* and consequently no human interaction is required to initialize the active contour model. However, one of the major drawbacks of these procedures is their very high computational load. Various deterministic algorithms based on DP or variational methods [4] have then been constructed for finding the optimal (minimum energy) contour in a neighbourhood of the initial contour.

Contrary to gradient ascent-based methods which use derivative measures, the DP-based optimization method determines the minimum of an energy function by a straightforward search technique. This procedure is especially well suited for the deformable contour minimization problem for which the optimization problem to be solved exhibits *optimal substructure* (i.e. the optimal solution contains within it optimal solutions to subproblems) and *overlapping subproblems* (i.e. the optimization problem revisits the same subproblem over and over again) [12]. We can indeed easily notice that energy function given in Eq. (1) can be written in terms of separate energy term, i.e. $E_1, E_2, \ldots, E_{n-2}$, such that each energy term E_i depends only

on v_{i-1}, v_i and v_{i+1}. More precisely, we have,

$$E_{\text{snake}}(v_1, v_2, \ldots, v_n) = E_1(v_1, v_2, v_3) + E_2(v_2, v_3, v_4) + \cdots + E_{n-2}(v_{n-2}, v_{n-1}, v_n), \quad (6)$$

where $E_{i-1}(v_{i-1}, v_i, v_{i+1}) = E_{\text{int}}(v_i) + \beta E_{\text{ext}}(v_i, y)$. In a DP-based optimization context, each variable v_i is allowed to take only m possible values, generally corresponding to adjacent "snaxel" locations within a search neighbourhood. Consequently, we can efficiently define the value of an optimal solution recursively in terms of the optimal solutions to the following optimization subproblems,

$$s_1(v_2, v_3) = \min_{v_1} \{E_1(v_1, v_2, v_3)\},$$

$$s_2(v_3, v_4) = \min_{v_2} \{s_1(v_2, v_3) + E_2(v_2, v_3, v_4)\},$$

...

$$s_{n-2}(v_{n-1}, v_n) = \min_{v_{n-2}} \{s_{n-3}(v_{n-2}, v_{n-1}) + E_{n-2}(v_{n-2}, v_{n-1}, v_n)\},$$

and finally, the optimal contour can be obtained by minimizing,

$$\arg \min_{\{v_i\}} E_{\text{snake}}(V) = \min_{v_{n-1}, v_n} s_{n-2}(v_{n-1}, v_n). \quad (7)$$

Since each optimal value function is calculated by iterating on three contour elements and there are $(n-2)$ of them, the time complexity of DP algorithm is polynomial and is $O(nm^3)$. This recursive procedure constitutes a single iteration. For finding the final optimal contour the iterative process continues until $\arg \min_v E_{\text{snake}}(V)$ does not change between two iterations. The resulting contour produced the optimal contour if this one is contained within the initial search window because DP checks every possible alternative [12]. If this neighbourhood is too small and an unproper initialization of the initial contour is given, a local sub-optimal solution is then found. Nevertheless, if this search window is large enough, the optimal contour is then guaranteed, although at the expense of a significant increase of the computational complexity.

In order to shorten execution times for practical applications, researchers have recently suggested to combine DP algorithm with a multiresolution framework [5,13]. The main idea in using a multiresolution method is to allow to reduce the number of candidates in the search window, so that the research process gets faster. Deformable contour optimization algorithm is applied to the coarser resolution level and the obtained solution is used as the initial snake position for the next lower level. The process continues until the contour is optimized at the original image level. This procedure noticeably shorten the computational time. Nevertheless, the optimal solution is no more guaranteed. Besides, the construction of different resolution levels, usually obtained by low-pass filtering the data, results in losing some important information that our external energy term is sensitive to. In a region-based segmentation approach, this low pass-filter would change the nature and the parameter of the different PDFs exploited in the external energy term (see Eq. (4)). It is even more true if the PDFs are not Gaussian, which is our case in ultrasound imagery (see Section 5). At coarser levels, the optimization algorithm will converge towards a biased solution. The same problem remains valid for external energies using edges or textures. In these cases, the information used by the external energy can be altered or simply destroyed due to the filtering process.

In order to overcome these above mentioned problems, we propose to extend the discrete multiscale relaxation strategy combined with the multiresolution framework introduced by Heitz et al. in Ref. [6] for the minimization of our global energy function and also for all type of energy function associated to a dynamic contour. We consider this in the next section.

4. Multiscale minimization strategy

Instead of minimizing our global energy function directly on the full configuration space Ω, i.e. the space of possible contours, the optimization is led through a sequence of constrained configuration subspaces of increasing sizes,

$$\dim(\Omega^L) < \dim(\Omega^{L-1}) < \cdots < \dim(\Omega^0), \quad (8)$$

with $\Omega^0 \equiv \Omega$ and where Ω^l, $l = 0, \ldots, L$, designates the constrained configuration space at level l. At this resolution level, we choose to define V^l as a rough estimate of the contour model, defined by an ordered set of n_l nodes, $V^l = [v_{b_1^l}, v_{b_2^l}, \ldots, v_{b_{n_l}^l}]$ (with $V^0 \equiv V$ and $v_{b_i^0} \equiv v_i$), giving coordinates of points of this crude contour. Each point (or node) of this contour is indexed on a grid S^l which results from the reduction of S ($\equiv S^0$) by 2^l in each direction and is associated to the block of pixels $b_s^l \subset S$ of size $2^l \times 2^l$, "descendant" of node $v_{b_s^l}$ (see Fig. 2).

The constrained optimization in Ω^l of the original boundary detection problem is then equivalent to the minimization of the new energy function,

$$E_{\text{snake}}(V^l) = \sum_{i=1}^{n_l} (E_{\text{int}}(v_{b_i^l}) + \beta_l E_{\text{ext}}(v_{b_i^l}, y)). \quad (9)$$

Using a multigrid approach [6], we can easily define the external energy term $E_{\text{ext}}(v_{b_i^l}, y)$ involved in a region-based segmentation approach (see Eq. (4)) by,

$$E_{\text{ext}}(v_{b_i^l}, y) = -\frac{1}{N_{\text{in}}} \sum_{s \in v_{b_i^l}^{\text{in}}} \sum_{p \in b_s^l} \ln P_{\text{in}}(y_p) - \frac{1}{N_{\text{out}}} \sum_{s \in v_{b_i^l}^{\text{out}}} \sum_{p \in b_s^l} \ln P_{\text{out}}(y_p). \quad (10)$$

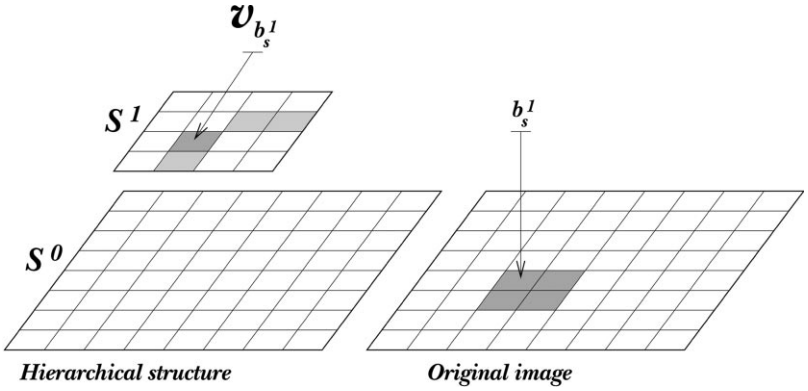

Fig. 2. Hierarchical structure ($L = 1$ in this example) involved in the multiscale minimization strategy and block of pixels b_s^l associated to the node $v_{b_s^l}$.

where the first summation ($\sum_{p \in b_s^l}$) is over the block of pixels b_s^l of size $2^l \times 2^l$, "descendant" of node $v_{b_s^l}$ (see Fig. 2) and the second summation ($\sum_{s \in v_{b_i^l}^{\text{in}}}$ and $\sum_{s \in v_{b_i^l}^{\text{out}}}$) is over all the N_{in} and N_{out} selected points belonging to the straight segment perpendicular to the contour at node $v_{b_i^l}$ (see Fig. 1).

In the same way, we can also define the external energy term $E_{\text{ext}}(v_{b_i^l}, y)$ involved in a classical edge-based segmentation approach (see Eq. (3)) by,

$$E_{\text{ext}}(v_{b_i^l}, y) = -\sum_{s \in b_i^l} \|\nabla y(v_s)\|. \tag{11}$$

which defines the external energy term at level l as the negative summation of the image gradient over the block of pixels b_i^l of size $2^l \times 2^l$ "descendant" of node $v_{b_i^l}$ (see Fig. 2).

The definition of $E_{\text{int}}(v_{b_i^l})$ remains similar to the one given in Eq. (2). However, one has to keep in mind that the angle between the two vectors has to be estimated on the reduced grid S^l. In addition, due to the size of each node at level l, we have $\beta = 4^l \beta_l$. From this family of energy functions, we are now able to define our minimization scheme as a cascade (from $l = L$ to $l = 0$) of optimization problems of reduced and increasing complexity, i.e.

$$V_{\text{opt}}^l = \arg \min_{\{v_i\}} E_{\text{snake}}(V^l), \qquad l = L, \ldots, 0. \tag{12}$$

These optimization problems are solved using a standard "coarse-to-fine" multigrid strategy. Starting from a coarse scale L, the optimization problem is first solved in Ω^L. This defines a first (crude) solution to the original problem and the obtained solution, a rough contour, is then used as the initial snake position for the next lower level. This process continues until the contour is optimized at the original image level (see Fig. 3). Contrary to standard multi-resolution approaches, no reduction of image data is applied. The family of defined energy functions uses the original image, ensuring that the same energy function (or more precisely, different smoothed versions of this energy function) is handled at each scale, and that the energy decreases at each step of the minimization process. This method has shown to exhibit fast convergence property and robustness against local *minima* for highly non-linear combinational problems [6]. Each of the associated energy minimization problems can be efficiently solved with a standard deterministic optimization algorithm, such as a classical gradient-based method or a DP algorithm requiring a small search window (and thus allowing to ensure the optimality of the solution). In the case of a region or a edge-based segmentation technique, we propose the two following strategies.

4.1. Region-based multiscale segmentation technique

For the minimization of each energy function (at each scale), we use simply the following iterative technique: for each node $v_{b_i^l}$ of the contour, we compute $E_{\text{snake}}(V^l)$ for the current position of the node and for the two consecutive points belonging to the perpendicular of the contour at the current node, respectively, located inside and outside the contour. At a given iteration, and for each node, we accept the position of the contour that minimizes $E_{\text{snake}}(V^l)$ and this process is iterated until there is no change in the shape of the contour between two iterations.

In our case, once the optimization problem at level l is solved, the initial snake position for the next lower level (level $l - 1$) is then obtained by keeping the descendant (among four) of each node ensuring the minimal external energy (see Fig. 3).

Finally, in order to initialize the model at the coarsest level $l = L$, we exploit the result of a two-class segmentation result achieved in a ML sense on the coarsest grid S^L.

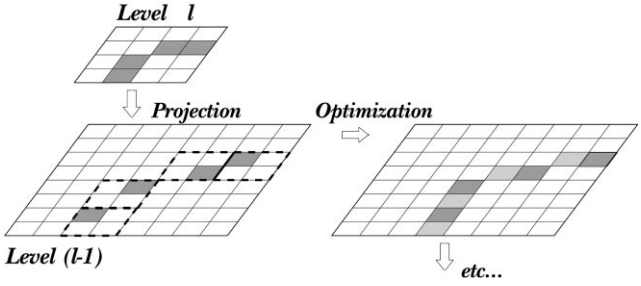

Fig. 3. "Coarse-to-fine" minimization strategy. The initial snake position for the next lower level is then obtained by keeping the descendant (among four) of each node ensuring the minimal external energy.

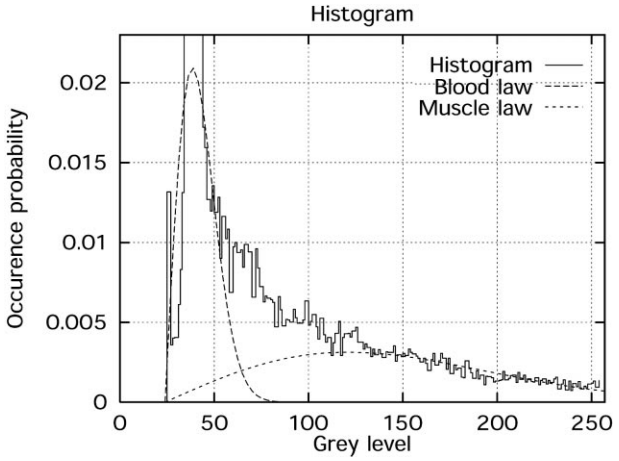

Fig. 4. Image histogram of the ultrasound image reported in Fig. 6 (solid curve) and estimated PDF mixture obtained with the ICE procedure (dashed and dotted curves).

To this end, let $x^L = \{x_s^L, s \in S^L\}$, the set of labels associated to each block of pixels b_s^L. Each x_s^L can take two labels $\{e_{\text{in}}, e_{\text{out}}\}$, associated to the two homogeneous regions and distributed according to the conditional distribution $P_{\text{in}}(y_s)$ and $P_{\text{out}}(y_s)$. This ML blocky segmentation is given by,

$$\forall s \in S^L, \qquad \hat{x}_s^L = e_{\text{in}}$$

$$\text{if} \sum_{p \in b_s^l} \ln P_{\text{in}}(y_p) > \sum_{p \in b_s^l} \ln P_{\text{out}}(y_p), \qquad \text{else, } \hat{x}_s^L = e_{\text{out}}.$$

This blocky segmentation is then high-pass filtered in order to extract the initial crude contour that will be used for the initialization of the optimization procedure at the coarsest level (see Section 5 and upper left of the pyramid reported in Fig. 6a).

4.2. Edge-based multiscale segmentation technique

In this case, a multiscale ML segmentation cannot be constructed and exploited in order to extract an initial contour. We have to initialize the initial snake position not *too far* from the optimal solution. A DP algorithm using a small search window then allows to ensure the optimal solution at the coarsest level $l = L$ and for the next higher resolution levels. Once the optimization problem at level l is solved, the initial snake position for the next lower level is then obtained by the strategy previously described (see Fig. 3). This process continues until the contour is optimized at the original level.

5. Experimental results

5.1. Ultrasound imagery

We have validated our region-based multiscale detection method on real echographic and echobrachial images, in order to detect the endocardial contour or the inner wall of an artery, respectively. For the experiments, we have chosen $\beta = 1$ for the weighting factor penalizing the internal energy with respect to the external energy and $L = 4$ for the number of resolution levels. The size of these acoustic pictures is 256×256 pixels (256 grey levels).

In order to take into account the speckle noise phenomenon [14] in the reverberation areas, we model the conditional PDFs $P_{\text{in}}(\cdot)$ and $P_{\text{out}}(\cdot)$ of each homogeneous region of the input ultrasound image by a shifted Rayleigh law with different parameters $\Phi = (\min, \alpha)$,

$$\mathcal{R}_Y(y_s; \min, \alpha) = \frac{y_s - \min}{\alpha^2} \exp\left(-\frac{(y_s - \min)^2}{2\alpha^2}\right), \qquad (13)$$

with $y_s > \min$ and $\alpha > 0$. The first region arises from the

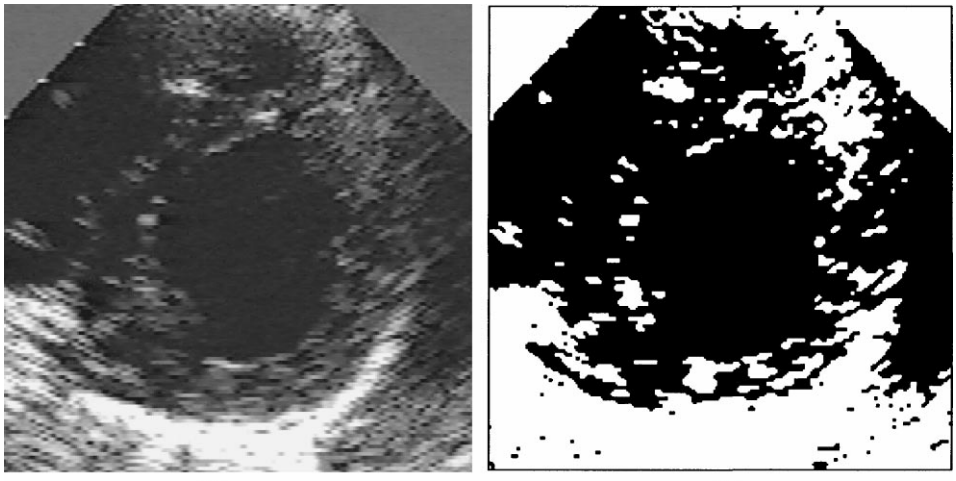

Fig. 5. Unsupervised Markovian segmentation of an ultrasound image using the single scale deterministic relaxation technique called ICM and based on the parameters estimated by the ICE procedure. (a) Real ultrasound image. (b) Two-class Markovian segmentation. The resulting segmented map exhibits unproper *blood* or *muscle* areas due to the strong speckle noise present in this image.

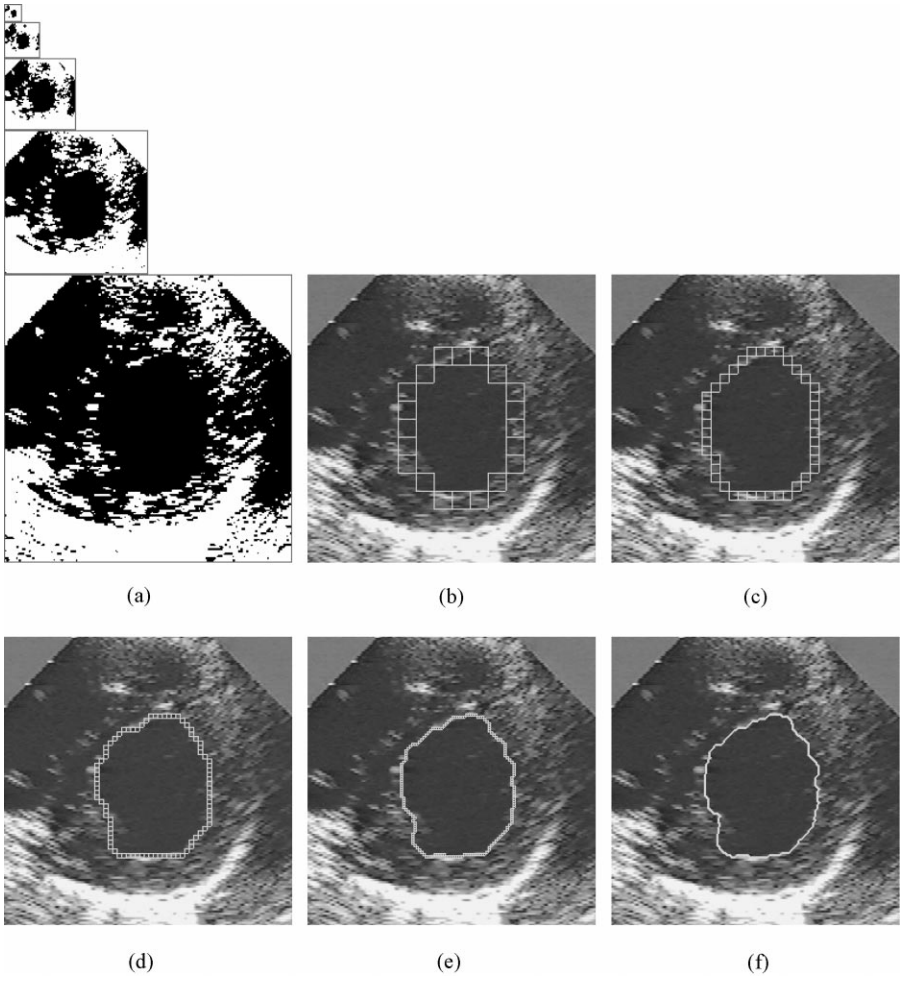

Fig. 6. (a) ML blocky segmentation at different resolution levels and estimated snakes at different resolution levels (b–f).

low acoustic wave reverberation in the different cavity of anatomical structures, generally filled with blood. The second region is due to the acoustic signal reverberation on the different organs (cardiac muscles for an echographic image, or wall of arteries for an echobrachial image). In our application, the parameter of these distribution laws are given by a preliminary statistical estimation method called iterative conditional estimation (ICE) [11]. Fig. 4 represents the distribution mixture estimated on the echogram shown in Fig. 5a and the histogram of this ultrasound image: the two conditional likelihoods (weighted by the estimated proportion π_i of each class) are superimposed to the image histogram. Corresponding estimates obtained by the ICE procedure are given in Table 1. Let us mention that this noise model estimation and the discussed unsupervised region-based segmentation procedure can easily be generalized for segmentation of anatomical structures in medical images exhibiting more than two classes.

Fig. 6a (at upper left) shows the ML blocky segmentation at the coarsest resolution level $l = L$ that is used to extract the initial crude endocardial contour. Fig. 6(b)–(f) shows the resulting estimated snakes at different resolution levels. We can notice (cf. Fig. 6a) that the ML blocky segmentation maps exhibits unproper *blood* or *muscle* areas at lower levels (higher resolution levels) of the pyramidal structure due to artifacts created by the ultrasound imagery process. The boundary of the endocardial contour cannot be efficiently extracted on these lower levels. Nevertheless, a closed (but crude) contour can be efficiently extracted at the highest level of the pyramidal structure. This crude contour is then used for the initialization of the optimization process at the coarsest level. The proposed multiscale strategy allows efficiently to obtain a good initial guess at each level that is refined at the finer scales (see Fig. 6(a)–(f)). Finally, a reliable detection of the

Table 1
Estimated parameters for the ultrasound image reported in Fig. 6. π stands for the proportion of the two classes within the image. *min* and α are the shifted Rayleigh law parameters

ECI procedure			
Φ_{in}	$0.48_{(\pi)}$	$24_{(min)}$	$207_{(\alpha^2)}$
Φ_{out}	$0.52_{(\pi)}$	$24_{(min)}$	$9436_{(\alpha^2)}$

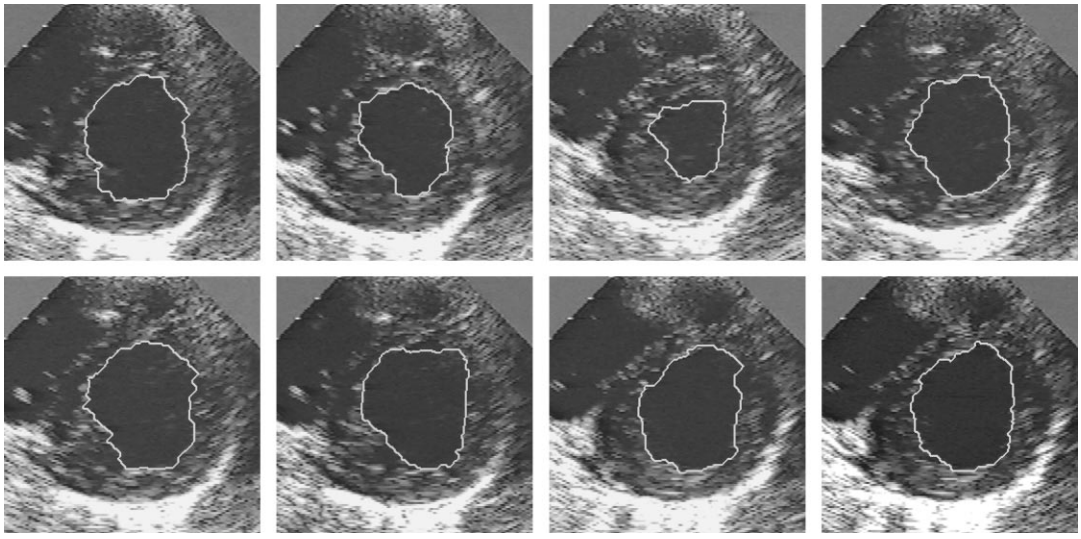

Fig. 7. Detection of the endocardial contour at different time frames during the cardiac cycle.

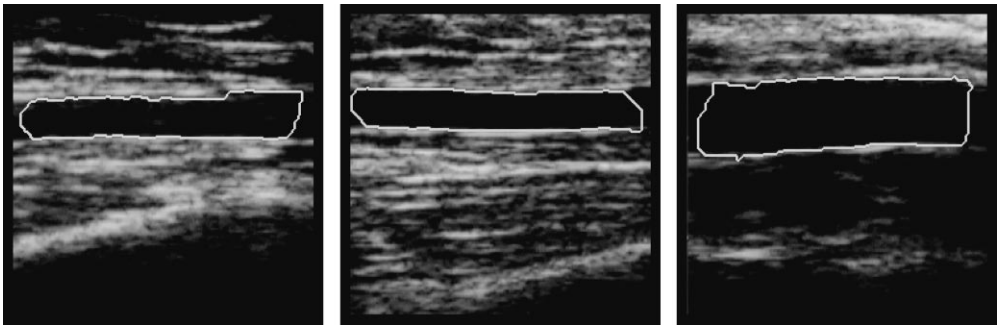

Fig. 8. Detection of the inner wall of an artery on echobrachial images. On these images, the a priori assumption, inherent to the snake model, that the structure to be detected has to be connected and the restricted size of each input image creates some artifacts on each side of the inner wall of the artery that has not to be taken into account.

endocardial contour or of the inner wall of an artery is obtained. Figs. 7 and 8 present the segmentation results obtained on other echographic images and on three echobrachial images, respectively. On these previous images, the a priori assumption, inherent to the snake model, that the structure to be detected has to be connected and the restricted size of each input image creates some artifacts on each side of the inner wall of the artery that has not to be taken into account. Finally, Fig. 9 shows a synthetic image presenting an object on a background with a strong synthetic speckle noise and the resulting segmentation obtained by our method. The proposed boundary segmentation procedure is very fast and takes about 2–3 s (average CPU time) on a standard Sun/Sparc 5 workstation which makes this procedure compatible with a practical application. Let us also mention that this procedure does not require to a priori fix the optimal number of nodes of the contour model.

In order to validate the accuracy and the speed of the proposed optimization method, we have compared the segmentation results obtained by a classical (single scale) DP-based optimization procedure. In the experiments, the initial endocardial contour which is used to initialize the DP procedure is the inner contour given by the coarser ML blocky segmentation and thus, this contour remains not *too far* from the optimal contour. In this context, the search window is defined by the set of eight points belonging to the straight segment perpendicular to the contour at each node and located inside and outside the contour. Segmentation result comparison is reported in Fig. 10 and show similar resulting boundary but at the expense of a ten times higher computational load (i.e. about 30 s).

We can also use this multigrid approach in order to define an efficient tracking procedure for dealing with ultrasound image sequence. An efficient tracking strategy consist in simply projecting the final highest resolution contour with a "fine-to-coarse" strategy and to use this new crude contour as an initialization of the multiscale optimization process for the next time frame. This multiscale tracking strategy has demonstrated to be more robust than the classical method, commonly used, that consist in using the final contour as an initialization for the next frame and that assumes

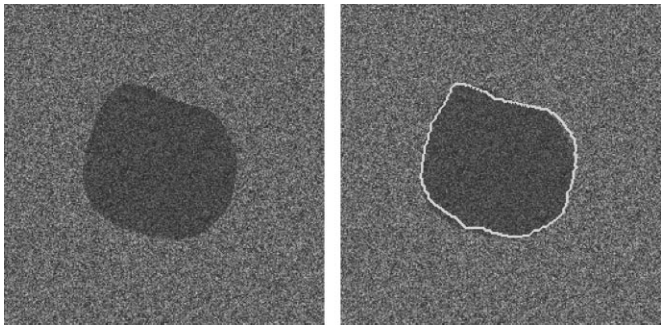

Fig. 9. Synthetic ultrasound image showing an object lying on a background with strong speckle noise and the resulting segmentation obtained by our method.

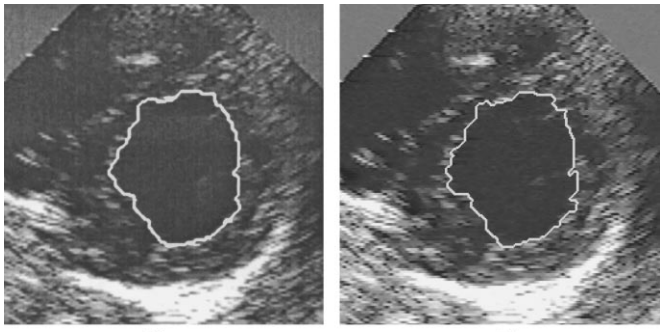

(a) (b)

Fig. 10. Segmentation result comparison between the proposed multiscale optimization procedure (a) and a classical single scale DP-based optimization procedure (b).

(sometimes wrongly) that the inter-frame motion is always small (cf. Fig. 7).

We can compare our results to those obtained by a Markovian segmentation of the ultrasound image in two classes (*blood*, *muscle*) based on the parameters estimation given by the ICE procedure. To this end, let now $X = \{X_s, s \in S\}$ be the label field. Each X_s takes its value in $\{e_0 = \text{blood}, e_1 = \text{muscle}\}$ and prior distribution $P_X(x)$ is now assumed to be stationary and Markovian. For the local a priori model, we adopt a standard isotropic Potts model with the eight-connexity spatial neighbourhood [1]. In this model, there are four parameters, called "the clique parameters" denoted $\beta_1, \beta_2, \beta_3, \beta_4$ and associated to the horizontal, vertical, right and left diagonal binary cliques, respectively [1]. Finally, in this framework, the segmentation issue can be viewed as a statistical labelling problem according to a global Bayesian formulation in which the following posterior energy has to be minimized [1],

$$U(x,y) = \underbrace{\sum_{s\in S} -\ln(P_{\text{in}}(y_s)\delta(x_s - e_0) + P_{\text{out}}(y_s)\delta(x_s - e_1))}_{U_1(x,y)} + \underbrace{\sum_{\langle s,t\rangle} \beta_{s,t}[1 - \delta(x_s, x_t)]}_{U_2(x)}, \qquad (14)$$

where U_1 expresses the adequacy between observations and labels, U_2 represents the energy of the a priori model and δ is the point Kronecker function. More precisely, the first term of energy, U_1, favours the blood label (and, respectively, the muscle label) in terms of likelihood (thanks to the preliminary estimation of the PDF of each class). The second term, U_2, corresponds to so-called Potts prior model which is extensively used in MRF-based segmentation techniques. It discourages segmentation with isolated labels and those with complex frontiers between regions. In our application, we use the following parameters: $\beta_{st} = \beta_1 = \beta_2 = \beta_3 = \beta_4 = 1$ according to the type of the clique $\langle s,t\rangle$ horizontal, vertical, right and left diagonal, respectively. We use the deterministic algorithm ICM [1] to minimize this global energy function. For the initialization of this algorithm, we exploit the segmentation map obtained by a ML segmentation (cf. Fig. 6a at higher resolution level). We can notice (cf. Fig. 5) that the resulting map exhibits unproper *blood* or *muscle* areas due to the strong speckle noise that creates open and/or ill defined contours. The boundary of the endocardial contour cannot be efficiently extracted by this method due to the unproper local prior model that does not assume that the object to be detected has to be connected.

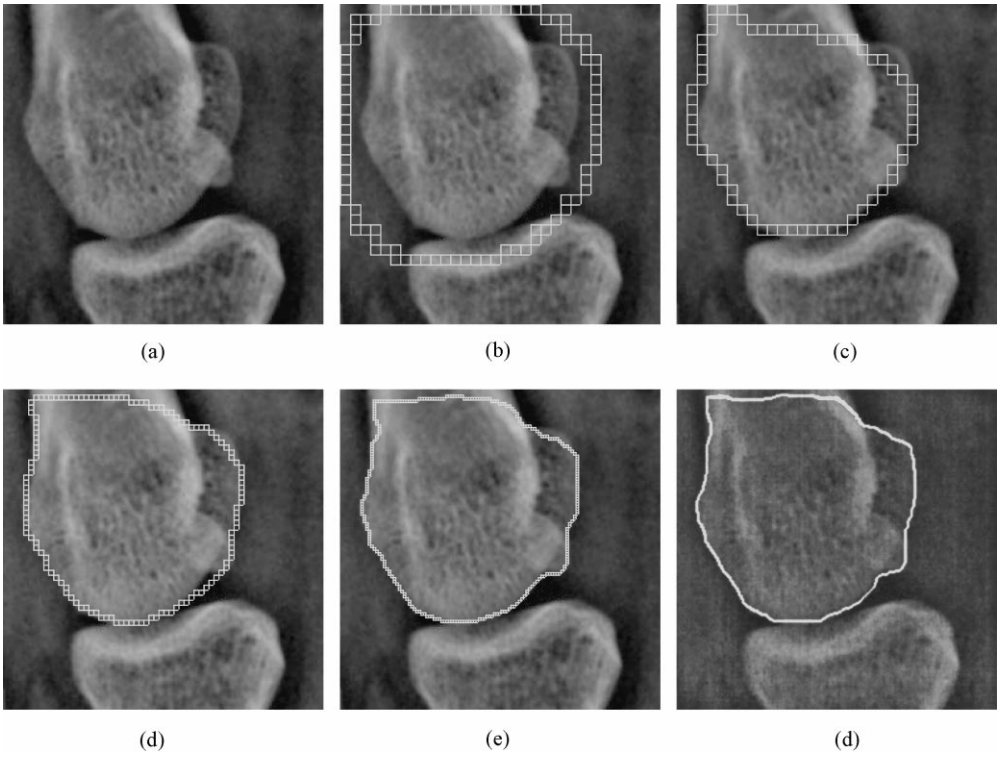

Fig. 11. (a) Radiographic medical image of a bone. (b) Initial snake position at coarsest level and estimated optimal snakes obtained by the DP-based multiscale optimization procedure at different resolution levels (c–f).

5.2. Radiographic imagery

Finally, we have validated our edge-based multiscale detection method (see Section 4.2) on real radiographic medical images in order to detect anatomical structures such as bones. For the experiments, we have chosen $\beta = 10$ for the weighting factor penalizing the internal energy with respect to the external energy and $L = 3$ for the number of resolution levels. The procedure is once again very fast about 1–2 s (average CPU time) on a standard Sun/Sparc 5 workstation and also twenty times faster than a classical single scale DP-based optimization procedure (cf. Fig. 11).

6. Conclusion

In this paper, we have developed a robust algorithm to detect the boundaries of anatomical structures, like the endocardial contour or the inner wall of arteries, in ultrasound images. We have stated this detection problem in the active contour model framework and we have taken into account the inherent smoothness of these structures and the grey level statistical distribution inside and outside the boundary of the object to be detected. We have finally presented a multiscale framework for the minimization of the global energy function resulting from this modelling. The minimization is efficiently performed through a multigrid algorithm, which consists in imposing successively weaker and weaker constraints on the searched estimate. In our application, this procedure results in estimating successively the optimal position of contour models of decreasing thickness. This framework can be used for edge-based segmentation technique and also easily generalized to texture-based energy-minimizing contour model as well as for three-dimensional boundary detection. This scheme is fast, exhibits good convergence properties, and is especially well suited to automatic extraction of anatomical structure boundaries in ultrasound imagery.

Acknowledgements

The authors thank NSERC (Natural Sciences and Engineering Research Council of Canada) for financial support of this work (postdoctoral grant). The authors are also grateful to Dr Francois Charbonneau (Royal Victoria Hospital) for having provided the echobrachial images and Dr Michel Bertrand (Ecole Polytechnique) and Dr Jean-Claude Tardif (Montreal Heart Institute) for the echocardiograms.

References

[1] Besag J. On the statistical analysis of dirty pictures. J R Stat Soc 1986;B-48:259–302.
[2] Hammoude A. Endocardial border identification in two-dimensional echocardiographic images: review of methods. Comput Med Imaging Graph 1998;22(3):181–93.
[3] Kass M, Witkin A, Terzopoulos D. Snakes: active contour models. IJCV 1988;1(4):321–31.

[4] Amini A, Weymouth T, Jain R. Using dynamic programming for solving variational problems in vision. IEEE Trans PAMI 1990;12(9):855–67.
[5] Geiger D, Gupta A, Costa LA, Vlontzos J. Dynamic programming for detecting, tracking and matching deformable contours. IEEE Trans PAMI 1995;17(3):294–302.
[6] Heitz F, Pérez P, Bouthemy P. Multiscale minimisation of global energy functions in some visual recovery problems. CVGIP: Image Understanding 1994;59(1):125–34.
[7] Chakraborty A, Staib LH, Duncan JS. Deformable boundary finding in medical images by integrating gradient and region information. IEEE Trans Med Imaging 1996;15:859–70.
[8] Geir Storvik. A Bayesian approach to dynamic contours through stochastic sampling and simulated annealing. IEEE Trans PAMI 1994;16(10):976–86.
[9] Williams DJ, Shah M. A fast algorithm for active contours and curvature estimation. CVGIP: Image Understanding 1992;55(1):14–26.
[10] Jain AK, Zhong Y, Lakshmanan S. Object matching using deformable templates. IEEE Trans PAMI 1996;18(3):267–78.
[11] Mignotte M, Meunier J. Deformable template and distribution mixture-based data modeling for the endocardial contour tracking in an echographic sequence. Proceedings of the CVPR, vol. 1, Fort Collins, CO, June 1999. p. 225–30.
[12] Coren TH, Leiserson CE, Rivest RL. Introduction to algorithms. MIT Press, 1990.
[13] Sinan Y, Kambhamettu C. A new multi-level framework for deformable contour optimization. Proceedings of the CVPR, vol. 2, Fort Collins, CO, June 1999. p. 465–70.
[14] Goodman JW. Some fundamental properties of speckle. J Opt Soc Am 1976;66(11):1145–50.

Max Mignotte received the PhD degree in Electronics and Computer Engineering from the University of Bretagne Occidentale (UBO) and the Digital Signal Laboratory (GTS) of the French Naval academy, France, in 1998. He was an INRIA post-doctoral fellow at University of Montreal (DIRO), Canada (Québec), from 1998 to 1999 and a NSERC post-doctoral fellow and a Lecturer at the University of Montreal from September 1999 to July 2000. He is currently with DIRO as an Assistant Professor at the University of Montreal. His current research interests include statistical methods and Bayesian inference for image segmentation (with hierarchical Markovian, statistical templates or active contour models), parameters estimation, tracking, classification, deconvolution and restoration issues in medical or sonar imagery.

Jean Meunier received the BSc degree in physics from the University of Montreal in 1981, the MSc a degree in Applied Mathematics in 1983, and PhD in Biomedical Engineering in 1989 from Ecole Polytechnique de Montréal. In 1989, after postdoctoral studies at the Montreal Heart Institute, he joined the Department of Computer Science at the University of Montreal, where he is currently a full Professor. He is also a regular member of the Biomedical Engineering Institute at the same institution. His research interests are in computer vision and its applications to medical imaging. His current research focuses on motion assessment and analysis in biomedical images.